# System energy optimisation strategies for metros with regeneration

Tian, Zhongbei; Weston, Paul; Zhao, Ning; Hillmansen, Stuart; Roberts, Clive; Chen, Lei

*DOI:*
10.1016/j.trc.2016.12.004



*Document Version*
Peer reviewed version

*Citation for published version (Harvard):*
Tian, Z, Weston, P, Zhao, N, Hillmansen, S, Roberts, C & Chen, L 2017, 'System energy optimisation strategies for metros with regeneration', Transportation Research. Part C, vol. 75, pp. 120-135. https://doi.org/10.1016/j.trc.2016.12.004

# System Energy Optimisation Strategies for Metros with Regeneration

Zhongbei Tian[a*], Paul Weston[a], Stuart Hillmansen[a], Clive Roberts[a], Ning Zhao[a], Lei Chen[a]

[a] School of Electronic, Electrical and Systems Engineering, University of Birmingham, Edgbaston, Birmingham, B15 2TT, U.K.

[*] Email: zxt279@bham.ac.uk

## Abstract

Energy and environmental sustainability in transportation are becoming ever more important. In Europe, the transportation sector is responsible for about 30% of the final end use of energy. Electrified railway systems play an important role in contributing to the reduction of energy usage and $CO_2$ emissions compared with other transport modes. For metro-transit systems with frequently motoring and braking trains, the effective use of regenerated braking energy is a significant way to reduce the net energy consumption. Although eco-driving strategies have been studied for some time, a comprehensive understanding of how regeneration affects the overall system energy consumption has not been developed. This paper proposes a multi-train traction power network modelling method to determine the system energy flow with regenerating braking trains, including the energy supplied from the substations, the energy wasted in the power transmission network, the energy used by the train in traction, and that regenerated by braking trains. The initial results show that minimising traction energy use is not the same as minimising the system energy usage in a metro system. The results of a study of the Beijing Yizhuang metro line indicate that optimised operation could reduce the energy consumption at the substations by nearly 38.6% compared to that used with the existing ATO operation.

*Keywords:* Energy-efficiency, traction, power network, regenerative braking, optimisation

## 1 Introduction

The railway system is one of the most efficient forms of land based transportation [1]. With the rapid increase in industry and populations in cities, metros are becoming an increasingly popular choice to satisfy transportation demand and reduce air pollution caused by car exhausts. However, despite the inherent efficiency, the energy used by the rail industry is high, making the study of railway energy efficiency of global importance.

There is a large and growing volume of literature concerning traction energy optimisation, as the traction energy usage accounts for around 60% to 80% of the total energy consumption for railway operation [2]. Chang proposed a genetic algorithm (GA) to optimise train speed profiles (running trajectories) using appropriate coasting control [3]. Both classical and

heuristic approaches are utilised in [4] to identify the necessary coasting points for a metro system. A heuristic method offers a faster and better solution for multiple coasting points compared with classical searching methods; and multi-coasting points control performs a better energy saving in a long interstation section than a single coasting point. In [5], the balance of energy consumption and journey time penalty are considered in the optimisation. Different searching algorithms, such as Ant Colony Optimisation, GA, and Dynamical Programming are compared in optimising single-train and multi-train trajectories in [6, 7]. It was found that Dynamical Programming performed better than both GA and ant colony optimisation in searching for energy-efficient driving styles. An analytical method was utilised to prove optimal driving strategies for routes with variable gradients in [8-10]. A numerical algorithm was proposed to calculate the optimal speed profiles by distributing the journey time into different sections, which achieved fast optimisation [11, 12].

With the development of regenerating trains, the use of regenerative braking energy has been studied widely. Optimisation of the train braking speed trajectory was studied to increase the total regenerative braking energy in a blended braking mode using the Bellman-Ford algorithm [13]. By optimising the braking speed trajectory, the regenerative braking energy can be increased by 17.23% compared with constant braking rate mode. Different scenarios were analysed to optimise Automatic Train Operation (ATO) speed profiles taking into account the energy recovered from regenerative trains [14, 15]. An integer programming model was formulated to improve overlapping time between the accelerating and braking trains by headway and dwell time control [16]. In [17], joint optimisation of the timetable and speed profile was illustrated using an integrated energy-efficient operation model by a GA. Energy- efficient dwell times were identified using a GA and an allocation algorithm, based on a metro system after traction energy optimisation [18].

However, the railway traction power network has largely been ignored in most previous studies of timetable scheduling, although the modelling of electrical power flow has been studied over many decades [19-23]. From the point of view of energy transfer, not all regenerated braking energy can be used by accelerating trains – some of it is lost in the power distribution resistance. The utilisation of regenerative braking energy depends on the distance between braking and motoring trains as well as on the tractive power demand. The effectiveness of regeneration must be solved using power flow analysis. Various iterative methods were proposed to solve the non-linear power flows in the traction power network with regenerating trains, such as Newton-Raphson iterative method, Point-Jacobi method, Zollenkopf's bifactorisation and incomplete Cholesky conjugate gradient (ICCG) methods [24-26]. Through the energy evaluation of a DC railway system with regenerating trains, the relationship between substation energy and headway for system with and without regenerating trains was illustrated [27, 28]. The results indicated that the substation energy consumption can be reduced by 22-44% when the regeneration is turned on. It was found that the available energy and substation energy demand vary with different headways and there is a 27% difference between the best and worst headways.

In this paper, an approach to optimise substation energy consumption by modifying interstation speed profiles and dwell times is proposed. A simulation method combining the vehicle motion and power network modelling is introduced and used as a tool to evaluate energy flow of DC railway system with regeneration. The system energy consumption statistic characteristics are studied and an 'energy factor' is defined to simplify the

optimisation. Finally, a case study based on Beijing Yizhuang Metro Line is used to illustrate the performance of the system energy optimisation algorithms.

# 2 Model formulation

## 2.1 Nomenclature

| | |
|---|---|
| $M$ | mass of the train [kg] |
| $\lambda$ | rotary allowance |
| $v$ | train speed [m/s] |
| $t$ | time [s] |
| $F$ | tractive effort applied at the wheels [N] |
| $g$ | acceleration due to gravity [m/s$^2$] |
| $\alpha$ | gradient angle [rad] |
| $F_R$ | resistance of motion [N] |
| $K$ | curvature resistance coefficient [Nm] |
| $r$ | radius of curvature of the track [m] |
| $A$ | Davis equation constant coefficient [N] |
| $B$ | Davis equation linear term coefficient [N/(m/s)] |
| $C$ | Davis equation quadratic term coefficient [N/$(\mathrm{m/s})^2$] |
| $N_T$ | total number of trains (each train runs one cycle) |
| $n$ | train index |
| $P_{mech\_n}$ | mechanical power at wheels for each train [W] |
| $P_{mech\_trac\_n}$ | mechanical tractive power for each train [W] |
| $P_{mech\_brake\_n}$ | mechanical braking power for each train [W] |
| $\eta$ | efficiency of electrical to mechanical conversion, and *vice versa* |
| $P_{elec\_trac\_n}$ | electrical tractive power for each train [W] |
| $P_{elec\_brake\_n}$ | electrical braking power for each train [W] |
| $P_{elec\_n}$ | electrical power requirement for each train [W] |
| $P_{aux}$ | train auxiliary power [W] |
| $E_{mech\_trac}$ | total mechanical tractive energy of trains [kWh] |
| $E_{mech\_brake}$ | total mechanical braking energy of trains [kWh] |
| $E_{traction}$ | total electrical tractive energy of trains [kWh] |
| $V_{t\_n}$ | instantaneous voltage of each train [V] |
| $I_{t\_n}$ | instantaneous current of each train [A] |
| $P_{final\_trac\_n}$ | actual electrical tractive power for each train [W] |
| $P_{final\_regen\_n}$ | actual electrical regenerative power for each train [W] |
| $E_{elec\_trac}$ | total actual electrical tractive energy of trains [kWh] |
| $E_{regen}$ | total actual regenerated braking energy of trains [kWh] |
| $E_{sub}$ | total substation energy consumption [kWh] |
| $E_{sub\_loss}$ | total substation energy loss [kWh] |
| $N_s$ | number of substations |
| $R_{sub}$ | substation equivalent source resistance [Ω] |
| $E_{trans\_loss}$ | total transmission energy loss [kWh] |
| $N_c$ | number of power transmission conductors |

| | |
|---|---|
| $R_n$ | resistance of conductor *n* [Ω] |
| $v_{ci}$ | coasting ending speed for each interstation journey [m/s] |
| $t_{di}$ | dwell time for each station [s] |
| $P_{overlap}$ | overlap power [W] |
| $E_{overlap}$ | overlap energy [kWh] |
| $C_r$ | regenerative energy coefficient |
| $E_{network\ loss}$ | network loss [kWh] |
| $C_n$ | network loss coefficient |
| $E_{sub\ est}$ | estimated substation energy consumption [kWh] |
| $\eta_{regen}$ | regeneration efficiency |

## 2.2 Energy flow in metro system

Metro systems are typically supplied from the national electricity grid, and use rectifier substations to convert AC voltage into 750, 1500, or 3000 V DC voltage to power the trains. Figure 1 shows the typical DC traction power network with multi-trains.

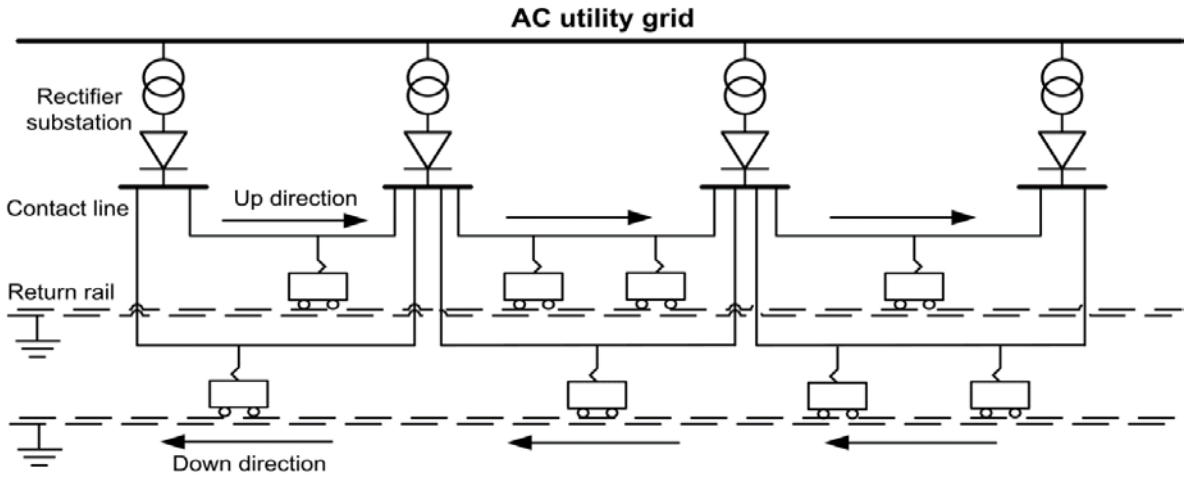


Figure 1- Typical DC traction power network with multiple trains

In order to study the energy efficiency of the whole system (up to the substations), typical energy consumption components with measured and estimated proportions are illustrated in Figure 2 [29]. If the sum of train traction and auxiliary energy is assumed as 100%, this amount of energy can be provided by substation energy (80%) and regenerative energy (30%), but around 10% is lost from substation and transmission losses. The mechanical energy at the wheels accounts for around 78%, as there is some energy loss transforming from electrical to mechanical energy. The mechanical energy can be transformed into kinetic and potential energy (63%) to move the train, but approximately 15% of the energy will be consumed by overcoming the resistance to motion. When a train is braking, the electrical braking mode can generate 45% electro-braking energy, and at the same time friction braking dissipates about 10% of the energy. Some of auxiliary system energy (5%) can be supplied by the electro-braking energy directly, and the remaining 10% auxiliary system energy is supplied from substation energy and regen energy together. Due to the overvoltage protection control, braking resistors dissipate 10% energy from the whole electro-braking energy and the remaining 30% regenerated energy can be fed back to the

catenary. In this paper, an approach to reduce substation energy consumption is proposed. In order to achieve the aim, train traction energy consumption is reduced and regenerated energy is increased by system optimisation.

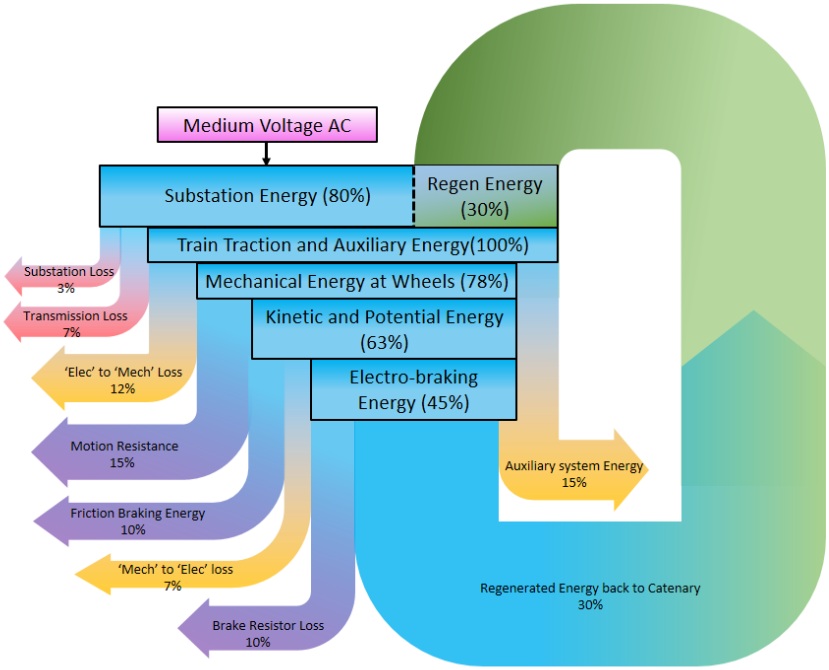


Figure 2- Typical energy flow chart in metro system

## 2.3 Simulator development

A simulator has been developed to evaluate the flow of energy in a railway system. The simulator is a composed of a single-train motion simulation and a multi-train power network simulation, as shown in Figure 3. Based on a specific railway route, the simulator can be used to evaluate energy flow according to different driving strategies and timetables.

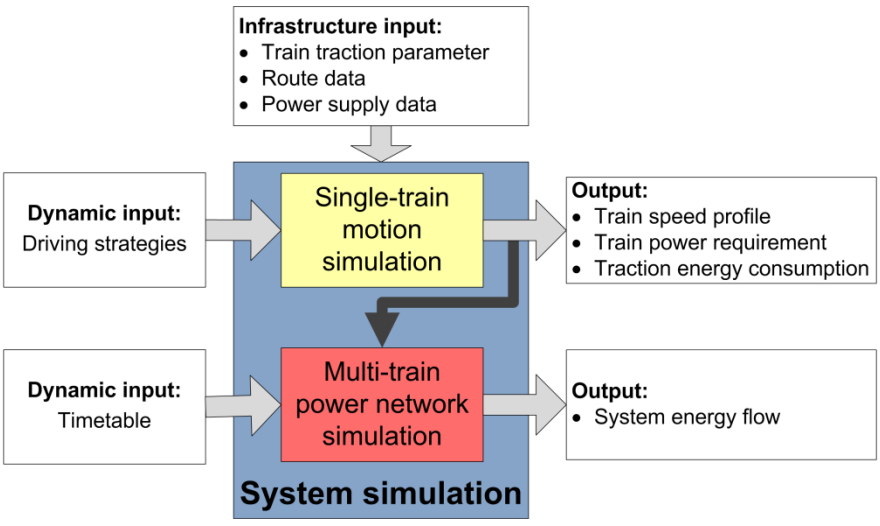


Figure 3- Simulator structure diagram

### 2.3.1 Single-train motion simulation

The train movement is determined by the standard Newtonian equations of motion. In the direction of travel, the motion of the vehicle is governed by tractive effort, gradient, the resistance to motion and the curvature resistance shown in equation (1).

$$M(1+\lambda)\frac{dv}{dt} = F - Mgsin(\alpha) - F_R - K/r \tag{1}$$

The resistance of motion is given by the Davis equation (2), where A, B and C are vehicle specific coefficients measured by run-down experiments [30].

$$F_R(v) = A + Bv + Cv^2 \tag{2}$$

The energy consumption can be computed according to the train speed trajectory. For each train $1 \leq n \leq N_T$, the mechanical power at the wheels is

$$P_{mech\_n}(t) = F_n(t)v(t) \tag{3}$$

The instantaneous train mechanical tractive and braking power can be converted from mechanical power at the wheels in equation (4a), which become positive values. The instantaneous train electrical tractive and braking power can be calculated from the mechanical tractive and braking power divided or multiplied by the efficiency, as appropriate, in equation (4b). The efficiency refers to the whole traction chain from current collector to the wheel, which is set at 85% in this paper.

$$\begin{cases} P_{mech\_trac\_n}(t) = \begin{cases} P_{mech\_n}(t) & if\ P_{mech\_n}(t) > 0 \\ 0 & if\ P_{mech\_n}(t) \leq 0 \end{cases} \\ P_{mech\_brake\_n}(t) = \begin{cases} \left|P_{mech\_n}(t)\right| & if\ P_{mech\_n}(t) < 0 \\ 0 & if\ P_{mech\_n}(t) \geq 0 \end{cases} \end{cases} \tag{4a}$$

$$\begin{cases} P_{elec\_trac\_n}(t) = P_{mech\_trac\_n}(t)/\eta \\ P_{elec\_brake\_n}(t) = P_{mech\_brake\_n}(t) \times \eta \end{cases} \tag{4b}$$

The auxiliary power is normally taken as a constant value $P_{aux}$. Therefore, the train electrical power requirement can be calculated by equation (5), which will be used in power network simulation. The train electrical power can be negative when the train is braking, and the electrical braking power is higher than auxiliary power.

$$P_{elec\_n}(t) = P_{elec\_trac\_n}(t) - P_{elec\_brake\_n}(t) + P_{aux} \tag{5}$$

The total mechanical traction energy required and mechanical braking energy produced by all the trains are

$$\begin{cases} E_{mech\_trac} = \sum_{n=1}^{N} \int_0^T P_{mech\_trac\_n}(t)\, dt \\ E_{mech\_brake} = \sum_{n=1}^{N} \int_0^T P_{mech\_brake\_n}(t)\, dt \end{cases} \quad (6)$$

The electrical traction energy requirement can be expressed by the train traction power requirement:

$$E_{traction} = \sum_{n=1}^{N} \int_0^T P_{elec\_trac\_n}(t)\, dt \quad (7)$$

### 2.3.2 Multi-train power network simulation

A power network simulation is used to calculate the energy flow throughout the power network, including the usage of regenerative braking energy. Figure 4 is the equivalent electrical circuit of the DC traction power network shown in Figure 1. There are four rectifier substations, which are represented by an ideal voltage source in series with an equivalent source resistance and a diode. There are eight trains running in the network: five trains motoring and three braking. The train is modelled as a dynamic power unit [27], which is considered as power load when the train is motoring, or a power source when the train is braking. While motoring, the current flows from the contact line to the return rail. When braking, the current flows back into the contact line. The power conductors (including the return rails) are modelled as resistances.

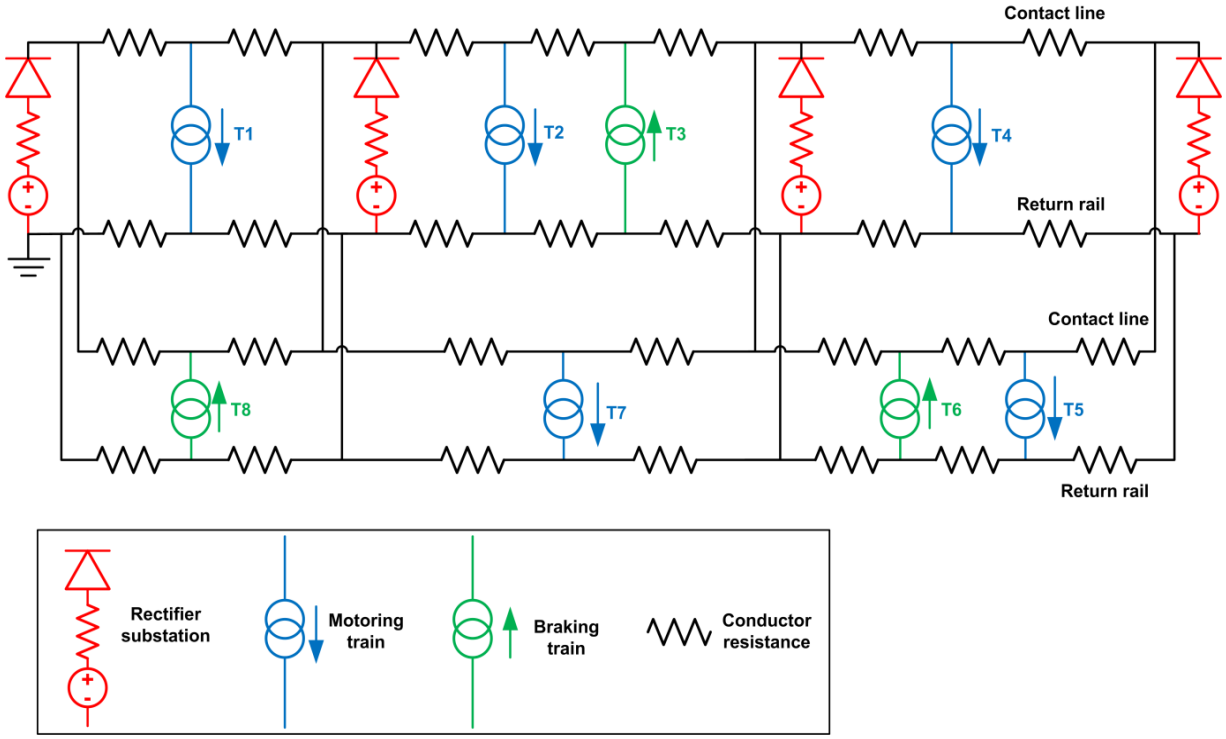


Figure 4- DC traction power network equivalent circuit

The movement of trains affects some the resistances in the electrical model, changing the admittance matrix $[Y]$. The power requirement of each train at any simulation time according to the specific driving strategy can be expressed as $P_{elec\_n}(t)$. An iterative method is applied to solve the nonlinear circuit with power sources and power loads. Firstly, each train voltage is initialised as the substation no-load voltage in (8).

$$V_{t\_n}^{(0)} = V_{sub\_no\_load} \tag{8}$$

Equations (9) are iterated until convergence.

$$\begin{cases} I_{t\_n}^{(k+1)} = \dfrac{P_{elec\_n}}{V_{t\_n}^{(k)}} \\ \left[V^{(k+1)}\right] = [Y]^{-1} \times \left[I^{(k+1)}\right] \end{cases} \tag{9}$$

The train current and voltage converge and finally the product will be equal to the train power. More details of power flow analysis including the cases of over- or under-voltage can be found in [25] and [27]. After all of the nodal voltage and current are solved, the electrical tractive power provided from the substations and the electrical regenerative power fed back into catenary are computed as shown in equation (10).

$$\begin{cases} P_{final\_trac\_n}(t) = \begin{cases} \left|V_{t\_n}(t) \times I_{t\_n}(t)\right| & if\ I_{t\_n}(t) > 0 \\ 0 & if\ I_{t\_n}(t) \le 0 \end{cases} \\ P_{final\_regen\_n}(t) = \begin{cases} \left|V_{t\_n}(t) \times I_{t\_n}(t)\right| & if\ I_{t\_n}(t) < 0 \\ 0 & if\ I_{t\_n}(t) \ge 0 \end{cases} \end{cases} \tag{10}$$

Therefore, the final electrical tractive energy consumption and electrical regenerative braking energy are

$$\begin{cases} E_{elec\_trac} = \sum_{n=1}^{N} \int_0^T P_{final\_trac\_n}(t)\, dt \\ E_{regen} = \sum_{n=1}^{N} \int_0^T P_{final\_regen\_n}(t)\, dt \end{cases} \tag{11}$$

As the instantaneous voltage and current of each substation are solved by power flow analysis, the substation energy consumption is then computed by integrating all substation instantaneous power over the time, as shown in equation (12).

$$E_{sub} = \int_0^T \sum_{n=1}^{N_s} (V_{sub_n}(t) \times I_{sub_n}(t))\, dt \tag{12}$$

The electrical losses within each substation is determined by the losses in the transformer and diodes [27]. However, as the substation loss does not have a significant effect on the system optimisation, for simplicity, the substation loss is approximated using the equivalent substation inner resistance shown in equation (13). The transmission loss can be calculated by each conductor resistance and the current through it, which is shown in equation (14).

$$E_{sub\_loss} = \int_0^T \sum_{n=1}^{N_s} (R_{sub} \times (I_{sub_n}(t))^2)\, dt \tag{13}$$

$$E_{trans\_loss} = \int_0^T \sum_{n=1}^{N_c} (R_n \times (I_n(t))^2)\, dt \tag{14}$$

# 3 Methodology

The frequent motoring and braking operations of a metro system makes the effective use of regenerative braking energy one of the most significant factors in energy saving methods. Therefore, timetable scheduling which affects the utilisation of regenerative braking energy has significant potential for energy-efficiency techniques in metro systems. Rather than optimising traction energy or regenerative braking energy, the substation energy consumption becomes the target of energy minimisation. With an increasing number of variables, solving the optimisation problem becomes increasingly difficult. Therefore, a statistical approach is introduced to solve system energy optimisation with large amount of variables.

## 3.1 Energy-efficient speed trajectory

Energy-efficient driving has been studied for a long time, and coasting control has been proved as an energy-efficient operation by the Pontryagin maximum principle [8-10] Train movement operation in this study includes motoring, cruising, coasting and braking. In the motoring mode, the maximal tractive effort is utilised which is always active at the beginning of the journey. The cruising mode is invoked when the train reaches the speed limit. During coasting, only auxiliary power is needed by the train and the speed only depends on the gradient and resistance to motion. Braking mode is applied when the train is approaching a stop or a lower speed limit. In this study, it is assumed that only electric braking is used in braking mode and the maximal electric braking effort is utilised for energy-efficiency [12].

Although multiple coasting points control achieve a better energy-efficiency in a long interstation journey, there is not enough room to accommodate multi-coasting commands for the metro system where the interstation distance is short [4]. Therefore, in this study, only one coasting point is utilised in the energy-efficient speed trajectory formulation. The travelling time between the successive stations is determined by the duration of cruising and coasting. For a given journey time there is a unique speed profile that can easily be identified. An example of possible driving speed profiles is shown in Figure 5. For each journey time, one speed trajectory can be generated by adjusting the cruising and coasting periods. If a shorter journey time is required, for example 129 s, the speed profile includes a long cruising and short coasting path. By contrast, if a longer journey time is required, for example 137 s, the speed profile includes only coasting path but no cruising path. For each journey with a distinct journey time, there is a unique final coasting speed. Therefore, the final coasting speed can be used as a variable to formulate the speed profile.

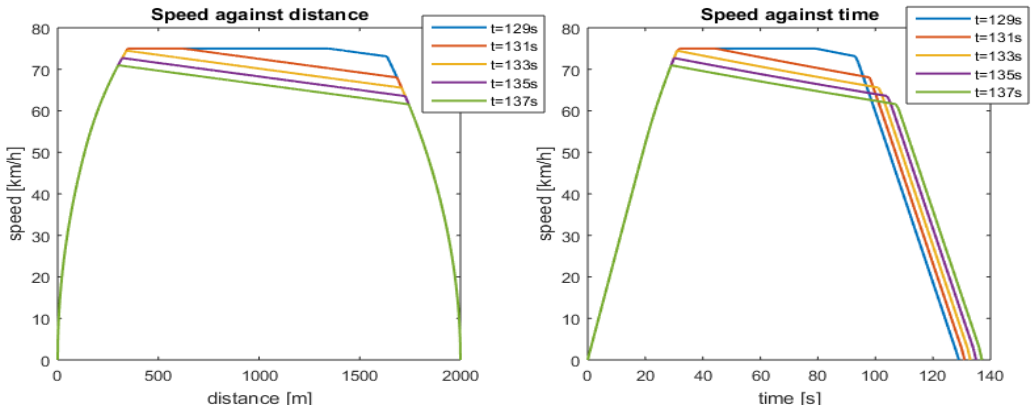


Figure 5- Acceptable energy-efficient speed profile

The permitted change of interstation journey time and dwell time from the nominal timetable is limited to 5 s, which is a reasonable range. The journey time and dwell times are assumed to be integers. The total running cycle time is the sum of each interstation travelling time and dwell time, as well as the turnaround time. The permitted difference of cycle journey time between the current operation and optimal operation is limited to 40 s. Turnaround time from up direction to down direction is assumed to be constant.

The combination of each interstation driving which meets the constraints is treated as one possibility. If the headway period is given, the substation energy consumption for the multi-train system can be calculated using the power network simulation. The coasting ending speed and each dwell time are used as variables in this optimisation. The substation energy can be expressed by

$$E_{sub} = f(v_{c1_{up}}, t_{d1_{up}}, v_{c2_{up}} \cdots v_{cn_{up}}, v_{c1_{down}}, t_{d1_{down}}, v_{c2_{down}} \cdots v_{cn_{down}}) \qquad (15)$$

## 3.2 System energy estimation

Trains in a metro system run repetitively and periodically when the headway is constant. During the headway period, each train of multi-train system finish one part of the cycle running, and the sum of each train running is the whole cycle journey. Therefore, sum of the each train's traction energy during the headway period is actually single train traction energy consumption of one cycle. The system energy evaluation for this study is always energy consumption during the headway period rather than that of the whole day's operation time.

The relationship between substation energy, traction energy consumption, and braking energy consumption is illustrated in Figure 6. Based on the Beijing Yizhuang line infrastructure data, 10,000 control sets were randomly selected from all possibilities. Each point in Figure 6 presents the traction and substation energy consumption or braking and substation energy consumption respectively. In each case, the full power flow solution was computed to find the energy used at the substations. Clearly, there is no linear relation between traction energy and substation energy or braking energy and substation energy. Therefore, minimising traction energy or braking energy does not generally minimise the substation energy.

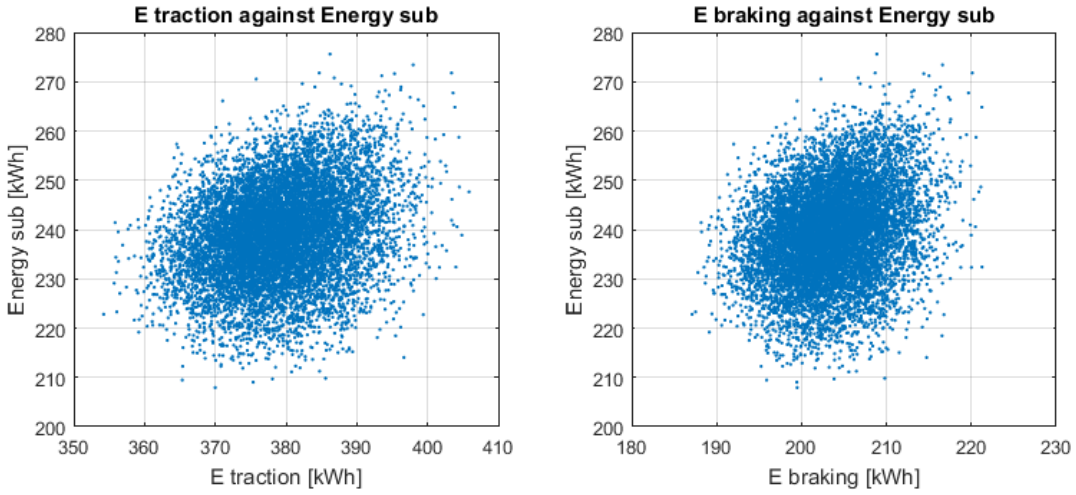


Figure 6- Substation energy compared with traction energy and braking energy

The objective of metro system energy optimisation is to minimise the substation energy consumption, which is given in equation (16). The substation energy can be only computed by power network simulator, which takes a significant time to solve the power flow analysis problem. Therefore, searching for the optimal control set with lowest substation energy from all possible controls is practically impossible. If it is possible to find a correlation between quantities that can be found quickly and the substation energy consumption, an 'energy factor', then this energy factor can replace the substation energy consumption to become the minimisation objective. In this way, this system energy optimisation problem can be solved by doing a full power flow analysis only on a limited number of candidate solutions that have been pre-selected according to some other easily computed quantity. It is, in effect, a heuristic.

$$E_{sub} = E_{elec\_trac} - E_{regen} + E_{trans\ loss} + E_{sub\ loss} \tag{16}$$

The concept of the overlap of traction power and braking power is proposed to solve the system energy optimisation problem. Overlap power is the minimum value of the sum of all tractive train power and sum of all braking train power at each time step, which is shown in equation (17). When there are higher tractive power requirement and the voltage level does not exceed the overvoltage protection limit, most of electrical braking power can be passed into the overhead line. One example of the traction power, braking power and regenerative power relation for all trains at different times is shown in Figure 7. The overlap power is never more than externally actual regenerated power. The overlap energy is the integral of overlap power over the time, shown in equation (18). The overlap energy can be used to predict the actual regenerative energy by multiplying a regenerative energy coefficient ($C_r$) shown in equation (19). The '$C_r$' can be obtained by the linear regression of overlap energy and actual regenerative energy under the whole system energy evaluation using Monte Carlo Simulation.

$$P_{overlap}(t) = min\left\{\sum_{n=1}^{N} P_{elec\_trac\_n}(t)\,,\ \sum_{n=1}^{N} P_{elec\_brake\_n}(t)\right\} \tag{17}$$

$$E_{overlap} = \int_0^T P_{overlap}(t)\, dt \tag{18}$$

$$E_{regen} = C_r \times E_{overlap} \tag{19}$$

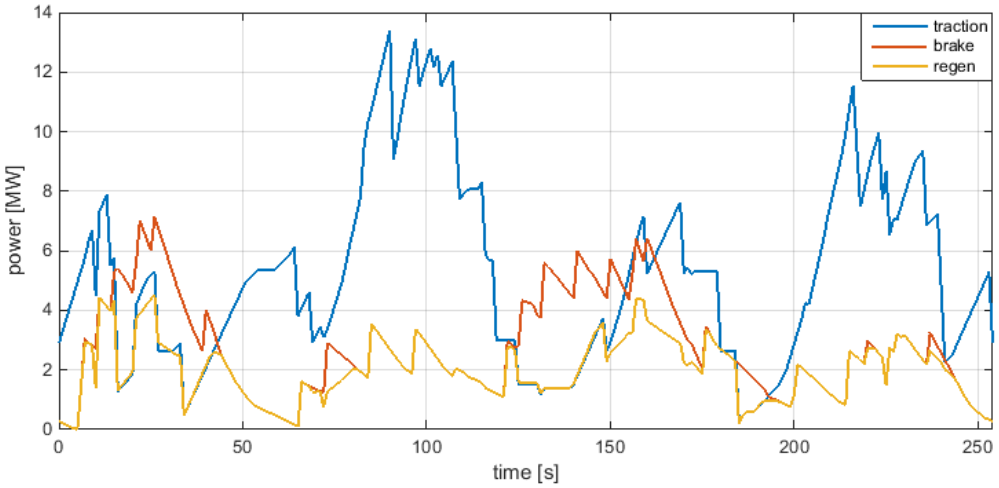


Figure 7- Tractive, braking and regenerative power relation

The sum of transmission loss and substation loss is the total power network energy loss shown in (20). The network loss coefficient ($C_n$) is used to characterise the relation between the substation energy and network energy loss in equation (21). The '$C_n$' can be obtained by the linear regression of substation energy and network energy under the whole system energy evaluation using Monte Carlo Simulation.

$$E_{network\ loss} = E_{trans\ loss} + E_{sub\ loss} \tag{20}$$

$$E_{network\ loss} = C_n \times E_{sub} \tag{21}$$

After initial system energy evluation using Monte Carlo Simulation, two coefficients '$C_r$' and '$C_n$' can be obtained based on the current route. These values are specific for a particular metro route and different values will be obtained if the headway, gradients, or distances between platforms are varied. The estimated substation energy can be expressed in equation (22) by using equation (16), (19), (20), and (21). And finally, the estimated substation can be calculated by equation (23). Only traction energy consumption and overlap energy are required, which can be obtained without power flow analysis.

$$E_{sub\_est} = E_{elec\_trac} - C_r \times E_{overlap} + C_n \times E_{sub\_est} \tag{22}$$

$$E_{sub\_est} = \frac{1}{1 - C_n} \times (E_{elec\_trac} - C_r \times E_{overlap}) \tag{23}$$

## 3.3 System energy optimisation

As the objective of the optimisation problem, the estimated substation energy is determined by each coasting velocity and dwell time, treated as variables. A Monte Carlo algorithm is used to choose variable combinations. All the possibilities are evaluated quickly by computing the estimated substation energy. After a large number of random choices have been evaluated, the best 100 possibilities are stored and fully evaluated using the power network simulation. Finally, the possibility with lowest substation energy consumption is identified. Naturally, being a statistical process, there is no guarantee that the best solution will be found, but because of the good correlation between estimated and actual substation energy, there is a good chance that a good solution will be found.

# 4 Case study

The Beijing Yizhuang metro line is used as a case study to illustrate the performance of system energy minimisation algorithm. The metro line covers a length of 22.73 km and contains 14 stations with both underground and over ground segments. There are 12 rectifier substations with nominal 750 V to power the network. For the power network simulation, the substation is modelled as an 850 V source in series with a $0.02\ \Omega$ resistance. A train driving strategies field test was conducted in September 2014 with no passengers. In order to compare with the field test results, the no-load train parameters are utilised in the simulation. Based on the field test measurement, the maximum service acceleration is measured as 0.8 $m/s^2$, and the maximum service braking rate is measured as 0.55 $m/s^2$. As a simplification, the auxiliary power is set to 0 kW. All the parameters under the actual train driving constrain are shown in Table 1. In this case study, the energy consumption during the peak hours is studied, where the headway is assumed as a constant with 254 s.

Table 1- infrastructure and vehicle parameters

| Item | Quantity | Units |
|---|---|---|
| Route length | 22.73 | km |
| Number of stations | 14 | |
| Number of substations | 12 | |
| Substation no-load voltage | 850 | V |
| Substation source resistance | 0.02 | Ω |
| Overvoltage limitation | 950 | V |
| Vehicle mass | 199 | tonnes |
| Passenger mass | 0 | tonnes |
| Max. tractive effort | 160 | kN |
| Max. tractive power | 2650 | kW |
| Auxiliary power | 0 | kW |
| Max. service acceleration | 0.8 | $m/s^2$ |
| Max. service deceleration | 0.55 | $m/s^2$ |

## 4.1 Current ATO timetable and energy consumption

Beijing Yizhuang metro trains are normally operated by an ATO system. Table 2 shows the current timetable and the energy consumption as measured by the ATO system during field tests. Each train travels from Yizhuang station to Songjiazhuang and back again, which is taken as one running cycle. It is usual that braking energy is lower than traction energy. However, in the 'up' direction, there is a steep uphill gradient between Ciqunan and Jinghailu, and a steep downhill gradient between Jiugong and Xiaohongmen. Thus, the electrical braking energy regenerated is lower than normal from Ciqunan to Jinghailu, and the electrical braking energy is even higher than traction energy from Jiugong to Xiaohongmen. There is a similar pattern for the 'down' direction.

**Table 2- Current ATO timetable and energy consumption in [kWh]**

| Index | 1 | 2 | 3 | 4 | 5 | 6 |
|---|---|---|---|---|---|---|
| Station | Yizhuang | Ciqu | Ciqunan | Jinghailu | Tongjinanlu | Rongchang |
| $t_{run}$ [s] | - | 105 | 101 | 140 | 148 | 160 |
| $t_{dwell}$ [s] | - | 45 | 35 | 30 | 30 | 30 |
| $E_{elec\_trac}$ | - | 17 | 15 | 34 | 21 | 23 |
| $E_{elec\_brake}$ | - | 6 | 11 | 9 | 12 | 13 |
| Index | 7 | 8 | 9 | 10 | 11 | 12 |
| Station | Rongjing | Wanyuan | Wenhuayuan | Yizhuangqiao | Jiugong | Xiaohongmen |
| $t_{run}$ [s] | 103 | 99 | 113 | 85 | 134 | 155 |
| $t_{dwell}$ [s] | 30 | 30 | 30 | 35 | 30 | 30 |
| $E_{elec\_trac}$ | 18 | 17 | 20 | 17 | 21 | 18 |
| $E_{elec\_brake}$ | 10 | 9 | 12 | 10 | 12 | 20 |
| Index | 13 | 14 | 13 | 12 | 11 | 10 |
| Station | Xiaocun | Songjiazhuang | Xiaocun | Xiaohongmen | Jiugong | Yizhuangqiao |
| $t_{run}$ [s] | 104 | 193 | 190 | 106 | 156 | 131 |
| $t_{dwell}$ [s] | 30 | 240(turnaround) | 30 | 30 | 30 | 35 |
| $E_{elec\_trac}$ | 21 | 25 | 25 | 14 | 32 | 22 |
| $E_{elec\_brake}$ | 10 | 11 | 12 | 8 | 10 | 11 |
| Index | 9 | 8 | 7 | 6 | 5 | 4 |
| Station | Wenhuayuan | Wanyuan | Rongjing | Rongchang | Tongjinanlu | Jinghailu |
| $t_{run}$ [s] | 86 | 112 | 100 | 103 | 163 | 147 |
| $t_{dwell}$ [s] | 30 | 30 | 30 | 30 | 30 | 30 |
| $E_{elec\_trac}$ | 16 | 15 | 16 | 15 | 19 | 21 |
| $E_{elec\_brake}$ | 11 | 11 | 9 | 10 | 10 | 11 |
| Index | 3 | 2 | 1 | | | |
| Station | Ciqunan | Ciqu | Yizhuang | **total** | | |
| $t_{run}$ [s] | 135 | 100 | 103 | **3271** | | |
| $t_{dwell}$ [s] | 35 | 45 | - | **1010** | | |
| $E_{elec\_trac}$ | 14 | 18 | 19 | **516** | | |
| $E_{elec\_brake}$ | 18 | 10 | 10 | **286** | | |

## 4.2 System energy estimation

Using the current timetable, all possible speed profiles that fulfil the interstation journey time constraint (including -5 to 5 s variants) are collected from motion simulator. 10,000 combinations of randomly chosen single train inter-station journeys and dwell times (with up to 5 s random variation) are evaluated by the power network simulator. The amount of overlap and regenerated energy for each combination is shown in Figure 8. A least-square

linear fit (forced through the origin) gives a regenerative coefficient '$C_r$' (the gradient) equal to 0.944. The Pearson correlation coefficient is 0.917, which denotes a very good linear relationship.

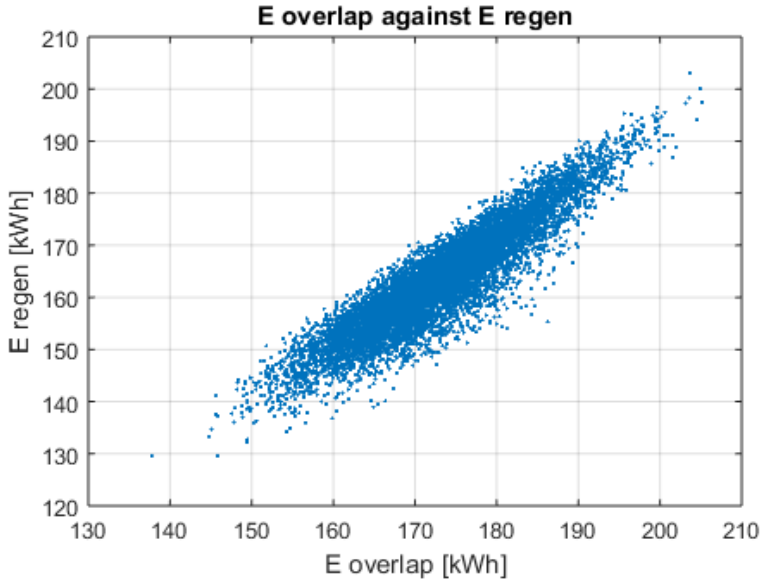


Figure 8- Regenerative braking energy compared with overlap energy

The substation energy and network loss results are shown in Figure 9. The Pearson correlation coefficient is 0.6447, which is smaller than the correlation between the overlap energy and regenerative energy. But, as the amount of network loss only accounts for about 10% of the substation energy, it is still a good estimation of network loss using network loss coefficient '$C_n$', which is 0.0986.

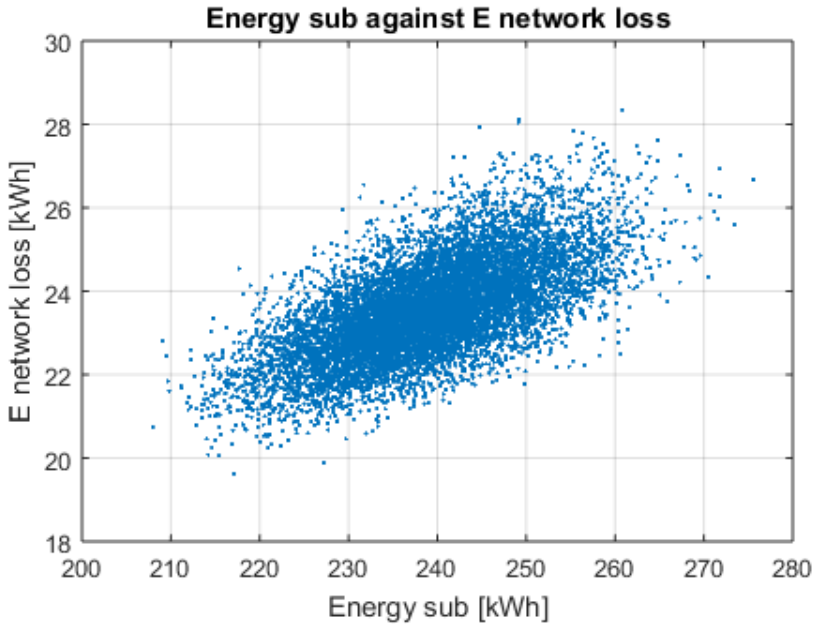


Figure 9- Network loss compared with substation energy

According to the regenerative and network loss coefficients, the estimated substation energy can be calculated using equation (23). Figure 10 shows the relationship between the

estimated substation energy and the actual substation energy. The correlation is 0.8615, which proves a significant linear relationship. The cumulative distribution function of the absolute errors of substation energy estimation is shown in Figure 11. The probability that the absolute error is lower than 5 kWh is about 70%, becoming 95% when the absolute error is less than 10 kWh. Therefore, estimated substation energy consumption is found very close to the actual value, which can then be used for optimising the system energy.

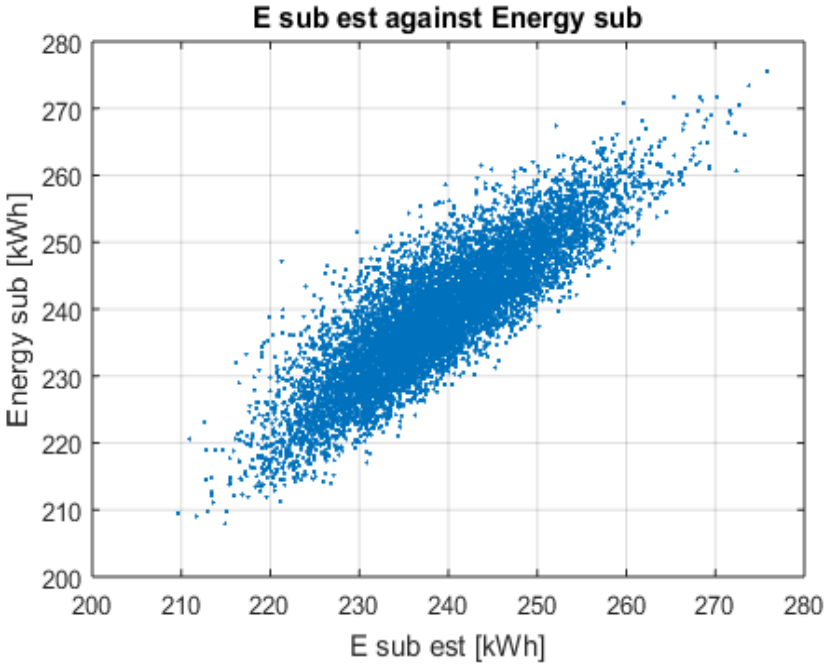


Figure 10- Estimated substation energy compared with actual substation energy

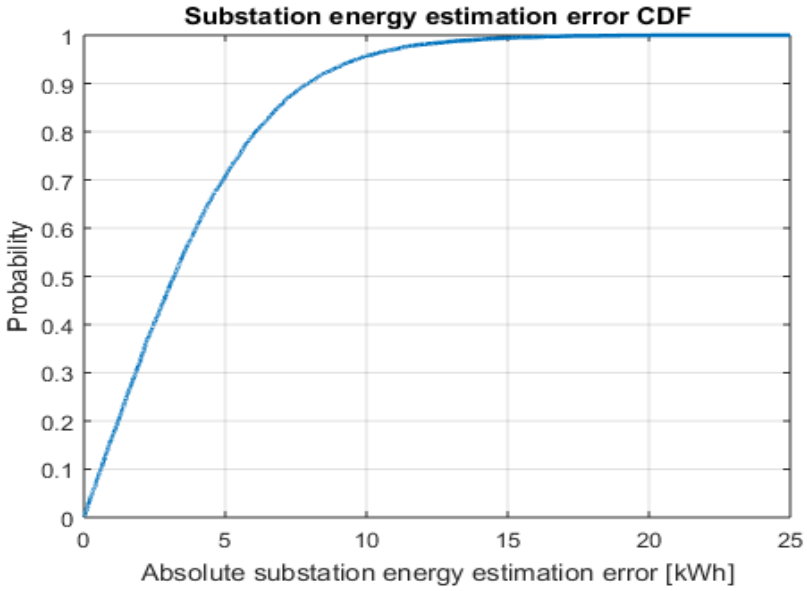


Figure 11- Substation energy estimation error cumulative distribution

## 4.3 System energy optimisation

Using the two coefficients obtained by Monte Carlo Simulation, the estimated substation energy of 500,000 random driving operation inputs are evaluated. It takes 3 minutes to calculate the estimated substation energy by a computer with 3.4 GHz CPU and 8 GB RAM. The algorithm stores the 100 cases with minimum estimated substation energy consumption. Figure 12 shows the lowest estimated substation energy is just below 205 kWh, and the decreasing rate of average energy of best 100 is very slow at 500,000 examples. A downward step occurs whenever better estimated substation energy consumption is found among the random samples. The mean estimated substation energy line is the average of the current best 100. This moves down a smoother path because sometimes one of the best 100 is replaced with better one and one drops out giving a lower mean.

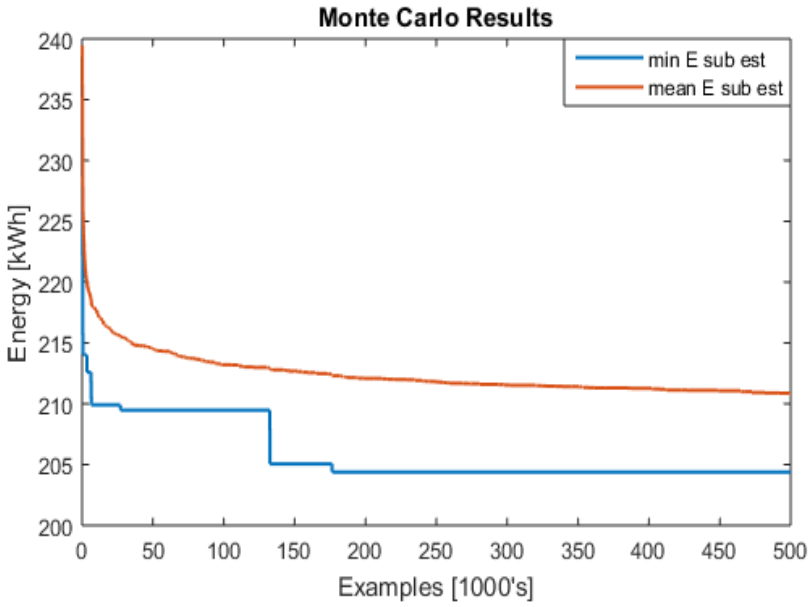


Figure 12- Monte Carlo estimated substation energy results

Finally, the best 100 examples are evaluated by the power network simulator. It takes around 3 seconds to calculate multi-train power flow for the headway period, so about 5 minutes to evaluate all 100 examples. All the 100 inputs show good substation energy consumption and 8 results with lowest substation energy consumption are shown in Table 3. The cycle journey time ranges from 4248 s to 4292 s, which results in slightly different traction energy. The regenerative efficiency which equals regenerative energy divided by electrical braking energy is defined by equation (24). Due to the short peak-hour headway, the regenerative efficiency of the top 8 results is very high, more than 90%. The traction energy, regenerative energy and energy loss affect the substation energy consumption together, but all of the top 8 examples show very good energy-efficiency.

$$\eta_{regen} = \frac{E_{regen}}{E_{elec\_brake}} \tag{24}$$

Table 3- Top 8 system energy optimisation results in [kWh]

| | **1** | **2** | **3** | **4** | **5** | **6** | **7** | **8** |
|---|---|---|---|---|---|---|---|---|
| $T_{cycle}$ [s] | 4248 | 4248 | 4289 | 4292 | 4291 | 4292 | 4290 | 4267 |
| $E_{sub}$ | 203.37 | 203.95 | 204.72 | 204.88 | 205.50 | 205.73 | 205.75 | 206.35 |
| $E_{sub\ loss}$ | 4.55 | 4.72 | 4.69 | 5.14 | 5.06 | 4.92 | 4.80 | 5.08 |
| $E_{trans\ loss}$ | 16.18 | 15.44 | 15.90 | 16.44 | 16.42 | 16.50 | 16.41 | 15.67 |
| $E_{traction}$ | 375.12 | 369.90 | 365.16 | 366.94 | 364.89 | 371.28 | 365.48 | 369.27 |
| $E_{elec\_brake}$ | 201.57 | 198.63 | 196.34 | 195.28 | 194.33 | 198.50 | 194.82 | 195.74 |
| $E_{regen}$ | 192.48 | 186.12 | 181.04 | 183.64 | 180.88 | 186.96 | 180.94 | 183.66 |
| $\eta_{regen}$ | 95.5% | 93.7% | 92.2% | 94.0% | 93.1% | 94.2% | 92.9% | 93.8% |

Table 4 illustrates the timetable and interstation energy consumption of the best solution found. All the optimised interstation journey times and dwell times as well as the single-train traction and braking energy are given. Compared with current ATO driving result in Table 2, the total journey time is reduced by 33 s, while the running time and dwell time are reduced by 6 and 27 s, respectively. At the same time, the traction energy consumption and electric braking energy are reduced by 27.5% and 29.7%, respectively. The resulting driving pattern is composed of acceleration, cruising, coasting and braking phases that could be implemented using ATO.

Table 4- Optimal driving timetable and energy consumption in [kWh]

| Index | 1 | 2 | 3 | 4 | 5 | 6 |
|---|---|---|---|---|---|---|
| Station | Yizhuang | Ciqu | Ciqunan | Jinghailu | Tongjinanlu | Rongchang |
| $t_{run}$ [s] | - | 106 | 100 | 144 | 143 | 162 |
| $t_{dwell}$ [s] | - | 44 | 38 | 25 | 33 | 33 |
| $E_{elec\_trac}$ | - | 9 | 13 | 27 | 19 | 14 |
| $E_{elec\_brake}$ | - | 6 | 8 | 4 | 10 | 6 |
| Index | 7 | 8 | 9 | 10 | 11 | 12 |
| Station | Rongjing | Wanyuan | Wenhuayuan | Yizhuangqiao | Jiugong | Xiaohongmen |
| $t_{run}$ [s] | 108 | 102 | 114 | 90 | 131 | 154 |
| $t_{dwell}$ [s] | 28 | 26 | 26 | 32 | 29 | 27 |
| $E_{elec\_trac}$ | 11 | 11 | 14 | 9 | 18 | 14 |
| $E_{elec\_brake}$ | 5 | 6 | 7 | 5 | 10 | 16 |
| Index | 13 | 14 | 13 | 12 | 11 | 10 |
| Station | Xiaocun | Songjiazhuang | Xiaocun | Xiaohongmen | Jiugong | Yizhuangqiao |
| $t_{run}$ [s] | 106 | 188 | 185 | 103 | 152 | 127 |
| $t_{dwell}$ [s] | 27 | 240(turnaround) | 30 | 33 | 25 | 32 |
| $E_{elec\_trac}$ | 11 | 13 | 12 | 11 | 28 | 19 |
| $E_{elec\_brake}$ | 6 | 4 | 5 | 7 | 7 | 10 |
| Index | 9 | 8 | 7 | 6 | 5 | 4 |
| Station | Wenhuayuan | Wanyuan | Rongjing | Rongchang | Tongjinanlu | Jinghailu |
| $t_{run}$ [s] | 87 | 108 | 104 | 99 | 161 | 144 |
| $t_{dwell}$ [s] | 29 | 28 | 35 | 27 | 30 | 26 |
| $E_{elec\_trac}$ | 9 | 16 | 10 | 15 | 13 | 19 |
| $E_{elec\_brake}$ | 6 | 10 | 6 | 10 | 7 | 9 |
| Index | 3 | 2 | 1 | | | |
| Station | Ciqunan | Ciqu | Yizhuang | **total** | | |
| $t_{run}$ [s] | 135 | 104 | 108 | **3265** | | |
| $t_{dwell}$ [s] | 36 | 44 | - | **983** | | |
| $E_{elec\_trac}$ | 16 | 11 | 9 | **374** | | |
| $E_{elec\_brake}$ | 20 | 6 | 4 | **201** | | |

According to the speed profile collected by ATO system, the system energy consumption can be computed by the power network simulation. The multi-train system energy consumption result is shown in Table 5, and compared with the optimised results. Table 5 shows the system energy consumption for three different operating regimes: the current ATO operation; the best identified by minimising the traction energy; and the best found by minimising the substation energy. The current ATO system energy consumption is calculated using a power network simulator using the speed profiles measured by the ATO system. It is found the simulated traction energy and braking energy is slightly higher than the measured energy consumption shown in Table 2 by about 1%, which is acceptable. The Traction optimisation column in Table 5 shows the energy consumption of the system under the traction optimisation but keeping the original timetable. The interstation journey times and dwell times are fixed and only one coasting point is used in each interstation journey. The results show that both traction energy and substation energy can be reduced by 29.9%. With traction optimisation alone, the regenerative efficiency (regenerative energy divided by braking energy) is almost the same as with ATO at 80.6% and 82.1%, respectively. The significant traction energy saving is probably because the motion simulator applies a perfect optimal speed trajectory which is not achieved in real world. Using substation energy optimisation, the traction energy consumption and braking energy is almost the same with the traction energy optimisation results, but the substation energy is reduced by an additional 10%. This is mainly caused by the higher regenerative efficiency which reaches 95.5%.

**Table 5- Optimisation results comparison**

| | Current ATO operation | Traction optimisation | System optimisation |
|---|---|---|---|
| Cycle running time [s] | 4281 | 4281 | 4248 |
| Substation energy per headway [kWh] | 331.28 | 232.21 | 203.37 |
| Substation loss per headway [kWh) | 12.38 | 6.41 | 4.55 |
| Transmission loss per headway [kWh] | 26.26 | 16.60 | 16.18 |
| Traction energy per headway [kWh] | 525.94 | 372.52 | 375.12 |
| Braking energy per headway [kWh] | 289.51 | 199.04 | 201.57 |
| Regenerative energy per headway [kWh] | 233.30 | 163.32 | 192.48 |
| Efficiency | 80.6% | 82.1% | 95.5% |

# 5 Conclusion

Because of the short interstation distance characteristic of a metro system, the trains accelerate and brake frequently. As a result, using the regenerative braking energy efficiently becomes an important factor in the metro system energy minimisation problem. The contribution of this paper is to propose an integrated energy optimisation approach to obtain energy efficient driving profile and timetable results for a DC metro system with regenerating trains. Both the vehicle motion and traction power network are modelled and simulated. To solve complex optimisation problem with lots of variables, the concept of estimation of substation energy consumption is defined. This energy estimation is utilised to simplify the progress of power flow analysis and reduce optimisation computing time. A Monte Carlo algorithm is utilised to identify the initial candidate solutions, acting as a

heuristic to guide the optimisation. Finally, the solutions that have been selected for further evaluation are simulated in a full power network simulation to identify the best energy-efficient operation.

The results in this paper show that the traction energy optimisation is not necessarily the best solution with the lowest system energy consumption at the substations. The case study based on Beijing Yizhuang Metro Line illustrates the performance of this integrated optimisation approach. Compared with the current ATO operation, the optimised operation within the time constraints can reduce the substation energy consumption by 38.6%, combining low traction energy consumption and high regenerative braking usage. The usage of regenerated energy accounts for 95.5% of the total electricity produced by electrical braking, which benefits from modifying the interstation travel time and dwell time.

Using this optimisation approach, not only one energy-efficient operation is identified, but numerous results with low energy consumption are found. The robustness can be studied by comparing different energy-efficient operations. The robustness to increases in real dwell times should be examined. Also, in this study, headway is assumed as a fixed value. It is known that headway is also an important factor in energy optimisation for a multi-train railway system, which is worth studying in the future.

# 6 Acknowledgment

This research is jointly supported by Guangzhou Metro Corporation and Guangzhou Metro Design & Research Institute Co., Ltd. Also, thanks are due to the financial support from Guangzhou Science and Technology Project (No. 201604030061), Anhui Birmingham International Research Institute in Rail Transportation and Anhui Comprehensive Transportation Research Institute.

# 7 Reference

[1] S. Hillmansen and C. Roberts, "Energy storage devices in hybrid railway vehicles: A kinematic analysis," *Proceedings of the Institution of Mechanical Engineers, Part F: Journal of Rail and Rapid Transit,* vol. 221, pp. 135-143, 2007.

[2] H. Douglas, C. Roberts, S. Hillmansen, and F. Schmid, "An assessment of available measures to reduce traction energy use in railway networks," *Energy Conversion and Management,* vol. 106, pp. 1149-1165, 2015.

[3] C. S. Chang and S. S. Sim, "Optimising train movements through coast control using genetic algorithms," *Electric Power Applications, IEE Proceedings -,* vol. 144, pp. 65-73, 1997.

[4] K. K. Wong and T. K. Ho, "Coast control for mass rapid transit railways with searching methods," *Electric Power Applications, IEE Proceedings -,* vol. 151, pp. 365-376, 2004.

[5] Y. V. Bocharnikov, A. M. Tobias, C. Roberts, S. Hillmansen, and C. J. Goodman,

"Optimal driving strategy for traction energy saving on DC suburban railways," *Electric Power Applications, IET,* vol. 1, pp. 675-682, 2007.

[6] S. Lu, S. Hillmansen, T. K. Ho, and C. Roberts, "Single-Train Trajectory Optimization," *Intelligent Transportation Systems, IEEE Transactions on,* vol. 14, pp. 743-750, 2013.

[7] C. S. Chang, A. Khambadkone, and X. Zhao, "Modeling and simulation of DC transit system with VSI-fed induction motor driven train using PSB/MATLAB," in *Power Electronics and Drive Systems, 2001. Proceedings., 2001 4th IEEE International Conference on*, 2001, pp. 881-885

[8] P. G. Howlett, "The Optimal Control of a Train," *Annals of Operations Research,* vol. 98, pp. 65-87, 2000.

[9] P. G. Howlett, I. P. Milroy, and P. J. Pudney, "Energy-efficient train control," *Control Engineering Practice,* vol. 2, pp. 193-200, 1994.

[10] R. Liu and I. M. Golovitcher, "Energy-efficient operation of rail vehicles," *Transportation Research Part A: Policy and Practice,* vol. 37, pp. 917-932, 2003.

[11] S. Su, T. Tang, X. Li, and Z. Gao, "A Subway Train Timetable Optimization Approach Based on Energy-Efficient Operation Strategy," *Intelligent Transportation Systems, IEEE Transactions on,* vol. 14, pp. 883-893, 2013.

[12] S. Su, T. Tang, X. Li, and Z. Gao, "Optimization of Multitrain Operations in a Subway System," *Intelligent Transportation Systems, IEEE Transactions on,* vol. 15, pp. 673-684, 2014.

[13] S. Lu, P. Weston, S. Hillmansen, H. B. Gooi, and C. Roberts, "Increasing the Regenerative Braking Energy for Railway Vehicles," *Intelligent Transportation Systems, IEEE Transactions on,* vol. 15, pp. 2506-2515, 2014.

[14] M. Domínguez, A. Fernández-Cardador, A. P. Cucala, and R. Pecharromán, R., "Energy Savings in Metropolitan Railway Substations Through Regenerative Energy Recovery and Optimal Design of ATO Speed Profiles," *Automation Science and Engineering, IEEE Transactions on,* vol. 9, pp. 496-504, 2012.

[15] M. Domínguez, A. Fernández-Cardador, A. P. Cucala, T. Gonsalves, and A. Fernández, "Multi objective particle swarm optimization algorithm for the design of efficient ATO speed profiles in metro lines," *Engineering Applications of Artificial Intelligence,* vol. 29, pp. 43-53, 2014.

[16] X. Yang, X. Li, Z. Gao, H. Wang, and T. Tang, "A Cooperative Scheduling Model for Timetable Optimization in Subway Systems," *Intelligent Transportation Systems, IEEE Transactions on,* vol. 14, pp. 438-447, 2013.

[17] X. Li and H. K. Lo, "An energy-efficient scheduling and speed control approach for metro rail operations," *Transportation Research Part B: Methodological,* vol. 64, pp. 73-89, 2014.

[18] X. Yang, A. Chen, X. Li, B. Ning, and T. Tang, "An energy-efficient scheduling approach to improve the utilization of regenerative energy for metro systems," *Transportation Research Part C: Emerging Technologies,* vol. 57, pp. 13-29, 2015.

[19] B. Mellitt, C. J. Goodman, and R. I. M. Arthurton, "Simulator for studying operational and power-supply conditions in rapid-transit railways," *Electrical Engineers, Proceedings of the Institution of,* vol. 125, pp. 298-303, 1978.

[20] B. Mellitt, Z. S. Mouneimne, and C. J. Goodman, "Simulation study of DC transit systems with inverting substations," *Electric Power Applications, IEE Proceedings B,* vol. 131, pp. 38-50, 1984.

[21] C. J. Goodman and L. K. Siu, "DC railway power network solutions by diakoptics," in *Railroad Conference, 1994., Proceedings of the 1994 ASME/IEEE Joint (in Conjunction with Area 1994 Annual Technical Conference)*, 1994, pp. 103-110.

[22] C. Goodman, "Modelling and Simulation," in *Railway Electrification Infrastructure and Systems, 2007 3rd IET Professional Development Course on*, 2007, pp. 217-230.

[23] M. Z. Chymera, A. C. Renfrew, M. Barnes, and J. Holden, "Modeling Electrified Transit Systems," *Vehicular Technology, IEEE Transactions on,* vol. 59, pp. 2748-2756, 2010.

[24] Y. Cai, M. R. Irving, and S. H. Case, "Modelling and numerical solution of multibranched DC rail traction power systems," *Electric Power Applications, IEE Proceedings -,* vol. 142, pp. 323-328, 1995.

[25] Y. Cai, M. R. Irving, and S. H. Case, "Iterative techniques for the solution of complex DC-rail-traction systems including regenerative braking," *Generation, Transmission and Distribution, IEE Proceedings-,* vol. 142, pp. 445-452, 1995.

[26] C. L. Pires, S. I. Nabeta, and J. R. Cardoso, "ICCG method applied to solve DC traction load flow including earthing models," *Electric Power Applications, IET,* vol. 1, pp. 193-198, 2007.

[27] Z. Tian, S. Hillmansen, C. Roberts, P. Weston, N. Zhao, L. Chen*, et al.*, "Energy evaluation of the power network of a DC railway system with regenerating trains," *IET Electrical Systems in Transportation,* vol. 6, pp. 41-49, 2016.

[28] Z. Tian, P. Weston, S. Hillmansen, C. Roberts, and N. Zhao, "System energy optimisation of metro-transit system using Monte Carlo Algorithm," in *2016 IEEE International Conference on Intelligent Rail Transportation (ICIRT)*, 2016, pp. 453-459.

[29] A. González-Gil, R. Palacin, P. Batty, and J. P. Powell, "A systems approach to reduce urban rail energy consumption," *Energy Conversion and Management,* vol. 80, pp. 509-524, 2014.

[30] B. P. Rochard and F. Schmid, "A review of methods to measure and calculate train resistances," *Proceedings of the Institution of Mechanical Engineers, Part F: Journal of Rail and Rapid Transit,* vol. 214, pp. 185-199, 2000.